Observation of Ultraslow Light Propagation in a Ruby Crystal at Room Temperature

Matthew S. Bigelow, Nick N. Lepeshkin, and Robert W. Boyd
The Institute of Optics, University of Rochester, Rochester, New York 14627
(Received 31 October 2002; published 21 March 2003)

We have observed slow light propagation with a group velocity as low as 57.5 ± 0.5 m/s at room temperature in a ruby crystal. A quantum coherence effect, coherent population oscillations, produces a very narrow spectral "hole" in the homogeneously broadened absorption profile of ruby. The resulting rapid spectral variation of the refractive index leads to a large value of the group index. We observe slow light propagation both for Gaussian-shaped light pulses and for amplitude modulated optical beams in a system that is much simpler than those previously used for generating slow light.

DOI: 10.1103/PhysRevLett.90.113903 PACS numbers: 42.65.–k, 42.50.Gy

There has recently been a flurry of interest in techniques that can allow the precise control of the velocity v_g of propagation of light pulses through material systems [1–3]. These techniques allow for the production of "slow" light ($v_g \ll c$) [4–7], "fast" light ($v_g > c$ or v_g negative) [8,9], and "stored" or "stopped" light [10,11]. Interest in these techniques lies at the level of both the fundamental understanding [12] of the physical laws that govern how fast or slow a light pulse can be made to propagate and the promise of new applications such as controllable optical delay lines, optical data storage, optical memories, and devices for quantum information.

It has been appreciated for quite some time that the group velocity v_g of an optical pulse propagating in a resonant optical material can differ significantly from the velocity c of light in vacuum. In these cases, the rapid change in the refractive index near a material resonance leads to a large value of the group index $n_g = c/v_g$ [13,14]. However, in these situations strong absorption accompanies the low group velocity, making the experimental observation of these effects difficult although not altogether impossible [15]. Most of the recent work on slow light propagation has made use of the technique of electromagnetically induced transparency (EIT) to render the material medium highly transparent while still retaining the strong dispersion required for the creation of slow light [16–18]. Using this technique, Kasapi *et al.* [4] observed a group velocity of $v_g = c/165$ in a 10 cm Pb vapor cell. More recently, Hau *et al.* [5] observed a group velocity of 17 m/s in a Bose-Einstein condensate and Kash *et al.* [6] used a modulation technique to measure a group velocity of 90 m/s in rubidium vapor. Using similar techniques, Budker *et al.* [7] inferred group velocities as low as 8 m/s. Also quite recently, Turukhin *et al.* [19] demonstrated the propagation of slow light with a velocity of 45 m/s through a solid-state material, Pr doped Y_2SiO_5, maintained at a cryogenic temperature of 5 K.

In this Letter, we report a new method that produces slow propagation of light in a solid-state material at room temperature. It entails the use of a different quantum coherence technique than that of the EIT concept, namely, the creation of a spectral hole due to population oscillations. This hole is created by the periodic modulation of the ground state population at the beat frequency between the pump and the probe fields applied to the material sample. The spectral hole created by this technique can be extremely narrow, 36 Hz in our experiment, and leads to a rapid spectral variation of refractive index and, consequently, to a group velocity as low as 57.5 ± 0.5 m/s.

These spectral holes due to coherent population oscillations were first predicted in 1967 by Schwartz and Tan [20] from the solution of the density matrix equations of motion and have been described in greater detail by subsequent authors [21–23]. In 1983, Hillman *et al.* [24] observed such a spectral hole in ruby. In their experiment, they used an argon-ion laser operating at 514.5 nm to pump population from the ground state to the broad $^4F_2$ absorption band. Population decays from this level within a few picoseconds to the metastable $2\overline{A}$ and $\overline{E}$ levels and eventually returns to the ground level with a decay time T_1' of a few milliseconds. As a result of this long lifetime, a spectral hole is created, centered at the laser frequency with a width of approximately the inverse of the population relaxation time. Hillman *et al.* [24] used modulation spectroscopy to observe this feature and measured its width to be 37 Hz.

Our experimental setup is shown in Fig. 1. We use a single-line argon-ion laser operating at 514.5 nm as the laser source. The beam passes first through a variable attenuator and then an electro-optic modulator. The modulator is driven by a function generator which allows us to either place a 6% sinusoidal amplitude modulation on the beam or produce long ($\sim$ ms) pulses with almost no background intensity. For all pulse lengths, these pulses had a peak power of 0.28 W with a background that was only 4% of that of the peak. A glass slide sent 5% of the beam to one detector for reference. The beam was then focused with a 40-cm-focal length lens to a beam waist of 84 μm near the front surface of a 7.25-cm-long ruby rod. Because the center of the beam experienced less

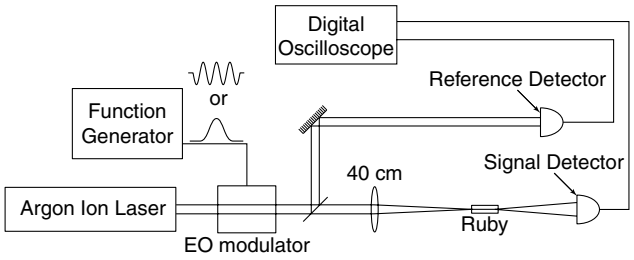

FIG. 1. The experimental setup used to observe slow light in ruby.

absorption than the edges due to saturation, the beam did not expand significantly in traversing the ruby. Ruby is a uniaxial crystal, and we rotated the rod to maximize the interaction. The beam exiting the ruby is incident on a detector, and the detected signal is stored along with that of the input beam on a digital oscilloscope. The resulting traces were compared on a computer to calculate the relative delay and amplitude of the two signals.

To analyze this situation mathematically, we refer to the ground state as level a, the $^4F_2$ absorption band as level b, and the levels $2\overline{A}$ and $\overline{E}$ as level c, as illustrated in inset (i) in Fig. 2. Because of the rapid decay of level b, it is possible to reduce this system to a two-level system shown in inset (ii). The density matrix equations of motion for this system are given by [25]

$$\dot{\rho}_{ba} = -\left(i\omega_{ba} + \frac{1}{T_2}\right)\rho_{ba} + \frac{i}{\hbar}V_{ba}w, \tag{1a}$$

$$\dot{w} = -\frac{w - w^{(\mathrm{eq})}}{T_1} - \frac{2i}{\hbar}(V_{ba}\rho_{ab} - V_{ab}\rho_{ba}), \tag{1b}$$

where w is the population inversion, $T_1 = 2T_1'$ is the

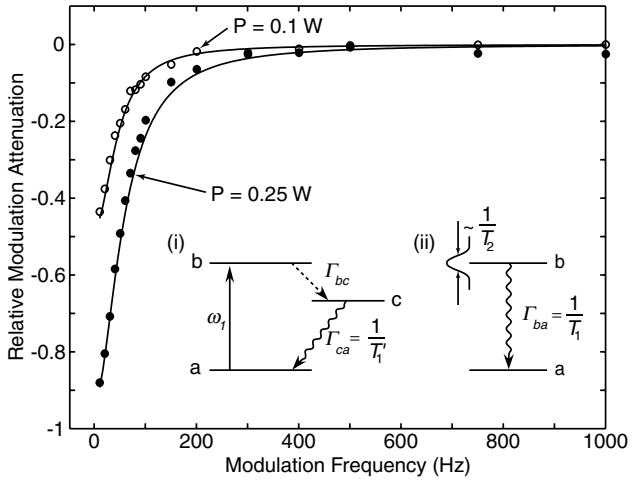

FIG. 2. The relative modulation attenuation $A(\delta)$ with respect to the pump as a function of modulation frequency for input pump powers of 0.1 and 0.25 W. The solid lines represent the theoretical model of Eq. (10). The insets show the two coupling schemes discussed in the text.

ground state recovery time, T_1' is the lifetime of level c, T_2 is the dipole moment dephasing time, and $w^{(\mathrm{eq})}$ is the population inversion of the material in thermal equilibrium. The distinction between T_1 and T_1' has been discussed by Sargent [21]. The interaction Hamiltonian in the rotating-wave approximation is given by $V_{ba} = -\mu_{ba}(E_1 e^{-i\omega_1 t} + E_3 e^{-i\omega_3 t})$, where E_1 and E_3 are the pump and probe field amplitudes, respectively, μ_{ba} is the dipole matrix element, and $\omega_3 = \omega_1 + \delta$. We seek a solution to the density matrix equation that is correct to all orders in the amplitude of the strong pump field and is correct to lowest order in the amplitude of the probe field. In this order of approximation, we represent the population inversion as

$$w(t) = w^{(0)} + w^{(-\delta)}e^{i\delta t} + w^{(\delta)}e^{-i\delta t}. \tag{2}$$

Rather complicated expressions for the quantities $w^{(0)}$, $w^{(-\delta)}$, and $w^{(\delta)}$ are given explicitly in Ref. [22], but the important conclusion is that the amplitudes of the population oscillations are appreciable only for $\delta \lesssim 1/T_1$. The response at the probe frequency can next be represented as [22]

$$\rho_{ba}(\omega_1 + \delta) = \frac{\mu_{ba}}{\hbar}\frac{E_3 w^{(0)} + E_1 w^{(\delta)}}{\omega_1 - \omega_{ba} + i/T_2}. \tag{3}$$

Note that the first term corresponds to the interaction of the probe wave with the static part of the population difference, whereas the second term represents the scattering of the pump wave off the temporally modulated ground state population. This contribution leads to decreased absorption at the probe frequency, that is, to a spectral hole in the probe absorption profile. To demonstrate this effect, we simplify Eq. (3) by assuming that $\omega_1 = \omega_{ab}$, that T_2^{-1} is large compared to the Rabi frequency $\Omega \equiv 2|\mu_{ab}||E_1|/\hbar$ and to the beat frequency $\delta \equiv \omega_3 - \omega_1$, and that $w^{(\mathrm{eq})} = -1$, to find

$$\rho_{ba}(\omega_1 + \delta) = \frac{i\mu_{ba}E_3T_2}{\hbar} \times \left(\frac{1}{1 + \Omega^2 T_1 T_2} - \Omega^2 \frac{T_2}{T_1}\frac{1 + i\delta/\beta}{\delta^2 + \beta^2}\right), \tag{4}$$

where the linewidth of the spectral hole (HWHM in angular frequency units) is given by

$$\beta = \frac{1}{T_1} + \frac{4T_2|\mu_{ab}|^2}{\hbar^2}(E_1^2) = \frac{1}{T_1}(1 + \Omega^2 T_1 T_2). \tag{5}$$

We can determine the linear susceptibility through use of Eq. (4) by means of the relation $\chi(\delta) = N\mu_{ba}\rho_{ba}(\omega_3)/E_3$ and, consequently, find expressions for the refractive index and the absorption experienced by the probe field as

$$n(\delta) = 1 + \frac{\alpha_0 c T_1}{2\omega_1}\frac{I_0}{1 + I_0}\left(\frac{\delta}{(T_1\delta)^2 + (1 + I_0)^2}\right), \tag{6}$$

$$\alpha(\delta) = \frac{\alpha_0}{1 + I_0}\left(1 - \frac{I_0(1 + I_0)}{(T_1\delta)^2 + (1 + I_0)^2}\right), \quad (7)$$

where $I_0 = I_1/I_{\text{sat}} \equiv \Omega^2 T_1 T_2$ is the normalized pump intensity and α_0 is the unsaturated absorption coefficient. Note that the second term in Eq. (7) is the spectral hole due to coherent population oscillations. We can calculate the group index as

$$n_g = n(\delta) + \omega_1 \frac{dn}{d\delta}. \quad (8)$$

This equation describes the propagation of spectrally narrow band pulses centered at the pump frequency ω_1. For broad band pulses, higher-order dispersion effects need to be taken into account [26]. Some of our experimental results were obtained through use of modulation techniques such that the optical field contained only a carrier wave (to act as the pump that creates the hole) and two sidebands (to act as probes). Since this field contains discrete frequencies rather than a continuum of frequencies, a generalized form of Eq. (8) describing the propagation of the modulation pattern through the material is given by $n_{\text{mod}} = n_1 + \omega_1[n(\delta) - n(-\delta)]/2\delta$, where n_1 is the refractive index experienced by the pump. Combining this with Eq. (6), we obtain

$$n_{\text{mod}} = n_1 + \frac{\alpha_0 c T_1}{2}\frac{I_0}{1 + I_0}\left[\frac{1}{(1 + I_0)^2 + (T_1\delta)^2}\right]. \quad (9)$$

For off-resonance modulations ($\delta \gg 1/T_1$), the modulation index reduces to $n_{\text{mod}} \approx n_1$. Similarly, the relative modulation attenuation [$A(\delta)$], defined as the difference between the attenuation of the modulation intensity and the attenuation of the pump intensity, is given by [21,24]

$$A(\delta) = \frac{1}{2}\ln\left[\frac{[1 + I_0(L)]^2 + (T_1\delta)^2}{[1 + I_0(0)]^2 + (T_1\delta)^2}\right], \quad (10)$$

where L is the length of the crystal.

To model the total group delay and modulation attenuation observed in our experiments, we first numerically calculated the value of I_0 throughout the length of the crystal. The pump beam intensity depends on the propagation distance through the ruby as

$$\frac{dI_0(z)}{dz} = -\frac{\alpha_0 I_0}{1 + I_0}. \quad (11)$$

Using the accepted value of 1.5 kW/cm^2 [27] for the saturation intensity of ruby at 514.5 nm, we integrate Eq. (11) numerically to find $I_0(z)$. Combining this function with our theoretical model for the dispersion, we could fit the total delay and the relative modulation attenuation measured in our experiment. We assumed α_0 and T_1 to be free parameters and found the values of $\alpha_0 = 1.17$ cm^{-1} and $T_1 = 4.45$ ms. These values are in the range found by Cronemeyer [28] and others. The total transmission in our experiments is on the order of 0.1%.

In Fig. 2, we show the measured relative modulation attenuation and compare it with the numerical solution of Eq. (10). In the limit in which the pump field becomes very weak, the spectral hole has a width of $1/(T_1 2\pi)$ or about 35.8 Hz (HWHM). As the input power is increased, the hole experiences power broadening. This result is in good agreement with the characteristics of the spectral hole that Hillman *et al.* [24] found in a 1 cm ruby.

This spectral dip causes an amplitude modulated beam to experience a large group index. We show the delay experienced by the modulation in Fig. 3 for input pump powers of 0.1 and 0.25 W. We observed the largest delay, 1.26 ± 0.01 ms, with an input pump power of 0.25 W, which corresponds in Fig. 2 to the power where the spectral hole is deepest but still very narrow. The inferred group velocity at this power is 57.5 ± 0.5 m/s. Note that the group velocity can be controlled by changing the modulation frequency or the input intensity. We found the nature of the effect to be strongly intensity dependent in that by moving the ruby a small distance from the focus we could greatly decrease the measured delay. As a check of our results, we found that the time delay would completely disappear if we moved the ruby far from the focus.

Moreover, we found that it is not necessary to apply separate pump and probe waves to the ruby crystal in order to observe slow light effects. A single intense pulse of light is able to provide the saturation required to modify the group index to provide slow light propagation. These relatively intense pulses can be thought of as producing their own pump field and are thus self-delayed. We know of no other examples where a separate pump beam is not required for generating ultraslow light. For this experiment, we used the programmable pulse generator

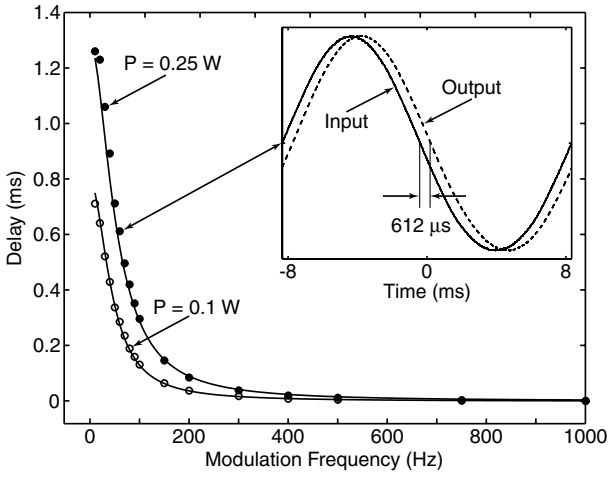

FIG. 3. Observed time delay as a function of the modulation frequency for input pump powers of 0.1 and 0.25 W. The solid lines represent the theoretical model of Eq. (9). The inset shows the normalized 60 Hz input (solid line) and output (dashed line) signal at 0.25 W. The signal was delayed 612 μs corresponding to an average group velocity of 118 m/s.

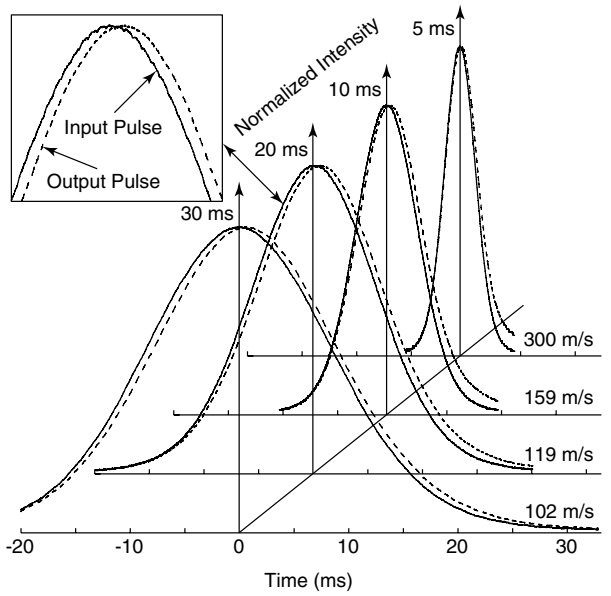

FIG. 4. The normalized input and output intensities of a 5, 10, 20, and 30 ms pulse. The corresponding average group velocities of the pulses are 300, 159, 119, and 102 m/s. The inset shows a close-up of the 20 ms pulse.

to produce Gaussian pulses with a $1/e$ intensity full width of 1 to 30 ms with almost no background, and we observed how they were delayed in propagating through the ruby. We found that the longer pulses also had the longer delays with the center of mass of a 30 ms pulse delayed by 0.71 ms with little pulse distortion. We show this result and those for other pulse lengths in Fig. 4. While the theory developed above, which assumed the presence of distinct cw pump and probe fields, does not model the pulsed experiment directly, that theory can be used to gain some intuition regarding the experiment. For instance, we would expect longer pulses, which contain lower frequency components, to experience longer delays.

In conclusion, we observed slow light propagation with a group velocity as low as 57.5 ± 0.5 m/s in a ruby crystal. In addition to seeing the amplitude modulation on a beam significantly delayed, we observed that single pulses without a pump background can also experience long delays. We have shown theoretically that these large group indices originate from a very narrow spectral hole in the homogeneously broadened absorption spectrum caused by coherent population oscillations. This technique for producing slow light is very easy to implement. It requires the use of only a single laser. In addition, since the location of the spectral hole follows exactly any drift in the laser frequency, the laser does not need to be frequency locked to any particular transition frequency. In fact, the laser does not even have to operate in a single longitudinal mode since all the modes will experience an identical delay. Also, since the slow light can be produced in a solid and at room temperature, this technique offers the possibility of applications in photonics such as fully integrated, controllable optical delay lines.

This work was supported by ONR Grant No. N00014-99-1-0539, ARO Grant No. DAAD19-01-1-0623, DOE Grant No. DE-FG02-01ER15156, AFOSR Grant No. F49620-00-1-0061, and the U.S. Department of Energy Office of Inertial Confinement Fusion under Cooperative Agreement No. DE-FC03-92SF19460 and the University of Rochester. The support of DOE does not constitute an endorsement by DOE of the views expressed in this article.

[1] R.W. Boyd and D. J. Gauthier, in *Slow and Fast Light*, Progress in Optics Vol. 43, edited by E. Wolf (Elsevier, Amsterdam, 2002).
[2] P.W. Milonni, J. Phys. B **35**, R31–R56 (2002).
[3] A. B. Matsko *et al.*, Adv. At. Mol. Opt. Phys. **46**, 191 (2001).
[4] A. Kasapi *et al.*, Phys. Rev. Lett. **74**, 2447 (1995).
[5] L.V. Hau *et al.*, Nature (London) **397**, 594 (1999).
[6] M. M. Kash *et al.*, Phys. Rev. Lett. **82**, 5229 (1999).
[7] D. Budker *et al.*, Phys. Rev. Lett. **83**, 1767 (1999).
[8] B. Segard and B. Macke, Phys. Lett. **109A**, 213 (1985).
[9] L. J. Wang, A. Kuzmich, and A. Dogariu, Nature (London) **406**, 277 (2000).
[10] C. Liu, Z. Dutton, C. H. Behroozi, and L.V. Hau, Nature (London) **409**, 490 (2001).
[11] D. F. Phillips *et al.*, Phys. Rev. Lett. **86**, 783 (2001).
[12] A. Kuzmich *et al.*, Phys. Rev. Lett. **86**, 3925 (2001).
[13] L. Brillouin, *Wave Propagation and Group Velocity* (Academic, New York, 1960).
[14] C. G. B. Garrett and D. E. McCumber, Phys. Rev. A **1**, 305 (1970).
[15] S. Chu and S. Wong, Phys. Rev. Lett. **48**, 738 (1982).
[16] S. E. Harris, J. E. Field, and A. Imamoglu, Phys. Rev. Lett. **64**, 1107 (1990); S. E. Harris, J. E. Field, and A. Kasapi, Phys. Rev. A **46**, R29 (1992).
[17] S. P. Tewari and G. S. Agarwal, Phys. Rev. Lett. **56**, 1811 (1986).
[18] R. S. Bennink *et al.*, Phys. Rev. A **63**, 033804 (2001).
[19] A.V. Turukhin *et al.*, Phys. Rev. Lett. **88**, 023602 (2002).
[20] S. E. Schwartz and T.Y. Tan, Appl. Phys. Lett. **10**, 4 (1967).
[21] M. Sargent III, Phys. Rep. **43**, 223 (1978).
[22] R.W. Boyd *et al.*, Phys. Rev. A **24**, 411 (1981).
[23] A. D. Wilson-Gordon, Phys. Rev. A **48**, 4639 (1993).
[24] L.W. Hillman *et al.*, Opt. Commun. **45**, 416 (1983).
[25] See, for instance, R.W. Boyd, *Nonlinear Optics* (Academic, San Diego, 1992).
[26] J. Peatross, S. A. Glasgow, and M. Ware, Phys. Rev. Lett. **84**, 2370 (2000).
[27] P. F. Liao and D. M. Bloom, Opt. Lett. **3**, 4 (1978).
[28] D. C. Cronemeyer, J. Opt. Soc. Am. **56**, 1703 (1966).